



Wang, Z., Tameh, EK., & Nix, AR. (2005). A sum-of-sinusoids based simulation model for the joint shadowing process in urban peer-to-peer radio channels. In *Vehicular Technology Conference 2005 (VTC 2005-Fall)* Institute of Electrical and Electronics Engineers (IEEE).
http://rose.bris.ac.uk:8080/dspace/bitstream/1983/169/1/wang_IEEE_VTC_Fall2005.pdf

Peer reviewed version

[Link to publication record in Explore Bristol Research](#)
PDF-document

University of Bristol - Explore Bristol Research

General rights

This document is made available in accordance with publisher policies. Please cite only the published version using the reference above. Full terms of use are available:
<http://www.bristol.ac.uk/red/research-policy/pure/user-guides/ebr-terms/>

A Sum-of-Sinusoids based Simulation Model for the Joint Shadowing Process in Urban Peer-to-Peer Radio Channels

Zhenyu Wang, Eustace K. Tameh and Andrew R. Nix

Centre for Communications Research, University of Bristol
Merchant Venturers Building, Woodland Road, Bristol, BS8 1UB, United Kingdom.
E-mail: {zhenyu.wang, tek.tameh, andy.nix}@bris.ac.uk

Abstract—Most conventional channel models are not capable of capturing the joint spatial correlation of shadowing processes between a large number of meshed radio channels in an ad-hoc wireless communications network. In this paper, we present a sum-of-sinusoids (SOS) based simulation model for the joint shadowing process in urban peer-to-peer radio channels. The performance of the proposed channel simulator is analyzed in terms of the autocorrelation and joint correlation function of the simulated shadowing process. Simulations illustrate that the proposed model is able to generate deterministic output shadowing values with a Normal distribution (in dB) and desired correlation properties. It is thus suitable for use in system level simulations, such as the evaluation of routing and radio resource management algorithms in ad-hoc networks.

I. INTRODUCTION

Ad-hoc and multihop networks are attracting significant levels of research interest in addition to being considered for beyond third generation wireless networks [1,2,3]. One of the core ideas in such networks is the provision of high capacity and connectivity through peer-to-peer (P2P) links. These short-range connections overcome heavy shadowing in the radio links and thus offer more efficient spatial reuse of the radio resources [1,3]. The need to evaluate the performance of routing protocols and radio resource management (RRM) schemes in such networks calls for channel models that properly reflect the cross spatial/temporal correlation properties of the shadowing process for meshed links between mobile nodes. It was reported in [4] that incomplete consideration of spatial correlation in multipoint-to-multipoint (M2M) radio channels (i.e. mobile to mobile) can lead to significant simulation errors, especially in the analysis of routing protocols and RRM.

Most existing shadowing correlation models [5,6,7,17] are established based on the base station (BS) to mobile station (MS) propagation channel for cellular networks, where only the MS moves. In [8], the cross-correlation of MS to multi-BS links is modelled for handoff performance studies. In [9], a general mathematical joint correlation model for shadow fading between two BS and two MS is derived. In the 3GPP Spatial Channel Model (SCM) [10], it is suggested to introduce correlation between channels from one mobile to two base stations by multiplying random Gaussian variables with a correlation matrix. However, these approaches are impractical when applied to P2P networks due to the large number of meshed channels between mobile nodes. In [10], the fast fading correlation between antenna elements in a MIMO channel is introduced by pre-generating a set of directional multipaths. This method is not suitable for generating correlated shadowing. In [4], a simple biased fading (random or site-specific) process

applied to each MS is suggested, but no detailed method is supplied. No efficient shadowing models are currently available in the literature to enable fast system level P2P simulations.

Among the existing methods for simulating fading channels, the sum of sinusoids (SOS) method has been shown to have many advantages, particularly in terms of accuracy and speed [7,11,12,13,14]. The SOS method is based on the fact that a Gaussian random process can be expressed as an infinite sum of sinusoids with random phases, and properly selected frequencies [15]. In practice, a finite number of sinusoids can be used to approximate a Gaussian process, which reduces complexity [11,12]. The statistical properties of SOS-based channel simulation models are presented in [12,13]. A fast implementation scheme based on a look-up table is advocated in [14]. In [11], the method of SOS is studied in more detail, and four different methods for the computation of the coefficients of the simulation model are developed. Three of these methods are applied to simulate the two-dimensional (2-D) shadowing process in [7].

In this paper, a SOS based simulation model is proposed for the joint shadowing process in urban P2P radio channels. A discrete Monte Carlo sampling method (DMCM) is used to determine the spatial frequencies of the sinusoidal waveforms according to the spatial power spectrum, which is calculated from the autocorrelation function (ACF) of the P2P link shadowing process. To distinguish between the 2-D ACF described in [7] and the 1-D ACF for a centralised link, the ACF of a P2P link is referred to in this paper as the joint-correlation function (JCF). The desired JCF was obtained in our previous publication [16] by making use of a detailed 3-D ray model. The performance of the resulting channel simulator is analyzed in terms of the average squared error (ASE) of the corresponding JCF relative to the theoretical desired JCF, the shadowing Cumulative Distribution Function (CDF), and the simulation speed.

II. CHANNEL MODEL AND SIMULATION METHODS

A. Shadowing Model

From various experimental results, it has been shown that the shadowing fluctuation can be characterized by a log-Normal distribution (i.e. the logarithm of a Normal distribution) over a large number of measurement locations with the same transmitter-receiver separation [17,18].

$$s(\mathbf{x}, \mathbf{y}, \mathbf{u}, \mathbf{v})[dB] = N(0, \sigma_{Shadow}) \quad (1)$$

where $N(\mu, \sigma)$ is a Gaussian/Normal distribution with mean μ and standard deviation σ . The shadowing fluctuation value s is a

function of the mobile location, with $[x, y]$ and $[u, v]$ denoting the positions of the mobiles at both ends of the P2P link (Tx and Rx). $s(x, y, u, v)$ can also be presented as a function of time $s(t)$, if the MSs are in motion.

The 1-D spatial ACF of the shadow fading is a measure of how fast the local mean power evolves as the MS at one end of the radio link moves along a certain route. This ACF can be modelled using an exponential decay function [5,6]:

$$R_1(d) = e^{\frac{-|d|}{d_{cor}} \ln 2} \quad (2)$$

where d is the distance moved by the MS, and the decorrelation distance d_{cor} , corresponds to the distance at which the correlation drops to 50%. Assuming that the shadowing fluctuation s is wide sense stationary, the ACF of s is now only a function of the distance of the MS movement. Hence (2) can be rewritten in the following form, where the movement vector $\mathbf{d} = [\Delta x, \Delta y]^T$:

$$R_1(\mathbf{d}) = e^{\frac{-|\mathbf{d}|}{d_{cor}} \ln 2} = e^{\frac{-\sqrt{\Delta x^2 + \Delta y^2}}{d_{cor}} \ln 2} \quad (3)$$

For the P2P radio channel, the shadowing JCF is a measure of how fast the local mean power evolves when the two MSs (i.e. Tx and Rx) at both ends of the link move around. It was found in [16] that the MS movement at each end of the P2P link has an independent and equal effect on the correlation coefficient. The JCF can be decomposed into two independent identical 1-D ACFs with respect to the movement of each MS, as shown in (4), where $\mathbf{d}_T = [\Delta x, \Delta y]^T$ and $\mathbf{d}_R = [\Delta u, \Delta v]^T$ denote the movement of the Tx and Rx respectively.

$$R_2(\mathbf{d}_T, \mathbf{d}_R) = R_1(\mathbf{d}_T) \cdot R_1(\mathbf{d}_R) \quad (4)$$

B. SOS Simulation Model

The simulation model for a Gaussian random process $s(t)$ based on the SOS method given in [11] is expressed as a 1-D function of the time variable:

$$\hat{s}(t) = \sum_{n=1}^N c_n \cos(2\pi f_n t + \theta_n) \quad (5)$$

where N is the number of sinusoids. Strictly speaking, when N is finite, the stochastic process $\hat{s}(t)$ is non-Gaussian distributed. But nevertheless the CDF of $\hat{s}(t)$ is close to a Gaussian density if N is sufficiently large, e.g. N ranging from 6 to 30 according to [11]. $\{\theta_n\}_{n=1}^N$ are random variables uniformly distributed in the range $[0, 2\pi]$. $\{f_n\}_{n=1}^N$ and $\{c_n\}_{n=1}^N$ are the sinusoid frequency set and the corresponding amplitude coefficients respectively, which are determined in a manner such that the resulting $\hat{s}(t)$ has similar statistical properties (e.g. the power spectral density - PSD -, which corresponds to the Fourier transforms of the ACF of the Gaussian random process [15]) to those of $s(t)$. Given that the only random variables in (5) are $\{\theta_n\}$, the ACF of $\hat{s}(t)$ can be evaluated as:

$$R_s(\Delta t) = E\{\hat{s}(t)\hat{s}(t + \Delta t)\} = \sum_{n=1}^N \frac{c_n^2}{2} \cos(2\pi f_n \Delta t) \quad (6)$$

In order to simulate the spatially correlated shadowing process of a P2P radio channel, we extend (5) to a 4-D spatial Gaussian process $s(x, y, u, v)$:

$$\hat{s}(x, y, u, v) = \sum_{n=1}^N c_n \cos(2\pi \mathbf{f}_n [x, y, u, v]^T + \theta_n) \quad (7)$$

where $\hat{s}(x, y, u, v)$ is the determined shadowing value on a virtual map characterized by the spatial frequency set $\{\mathbf{f}_n\}$, the corresponding coefficients $\{c_n\}$ and the phase $\{\theta_n\}$. The spatial frequencies $\{\mathbf{f}_n\} = [f_{x,n}, f_{y,n}, f_{u,n}, f_{v,n}]$ are vectors with four elements. We further define spatial frequencies $\mathbf{f}_{T,n} = [f_{x,n}, f_{y,n}]$, $\mathbf{f}_{R,n} = [f_{u,n}, f_{v,n}]$, $\mathbf{f}_T = [f_x, f_y]$, $\mathbf{f}_R = [f_u, f_v]$ and $\mathbf{f} = [f_x, f_y, f_u, f_v]$, for the convenience of subsequent referrals. The spatial frequency set $\{\mathbf{f}_n\}$ and the coefficients $\{c_n\}$ can be determined from the 4-D PSD of the Gaussian random process $s(x, y, u, v)$. To obtain the desired PSD, we need to perform the 4-D Fourier transform on the JCF in (4). This gives:

$$\begin{aligned} \Phi_2(\mathbf{f}) &= \Phi_2(\mathbf{f}_T, \mathbf{f}_R) = \int_{-\infty}^{\infty} \int_{-\infty}^{\infty} R_2(\mathbf{d}_T, \mathbf{d}_R) \cdot e^{-j(2\pi \mathbf{f}_T \cdot \mathbf{d}_T + 2\pi \mathbf{f}_R \cdot \mathbf{d}_R)} d(\mathbf{d}_T) d(\mathbf{d}_R) \\ &= \int_{-\infty}^{\infty} R_1(\mathbf{d}_T) \cdot e^{-j2\pi \mathbf{f}_T \cdot \mathbf{d}_T} d(\mathbf{d}_T) \int_{-\infty}^{\infty} R_1(\mathbf{d}_R) \cdot e^{-j2\pi \mathbf{f}_R \cdot \mathbf{d}_R} d(\mathbf{d}_R) \\ &= \Phi_1(\mathbf{f}_T) \cdot \Phi_1(\mathbf{f}_R) \end{aligned} \quad (8)$$

where $\Phi_1(\mathbf{f})$ and $\Phi_2(\mathbf{f}_T, \mathbf{f}_R)$ represent the Fourier transforms of the correlation functions $R_1(\mathbf{d})$ and $R_2(\mathbf{d}_T, \mathbf{d}_R)$ respectively. Equation (9) gives the 2-D PSD $\Phi_1(\mathbf{f}_T)$, (similarly for $\Phi_1(\mathbf{f}_R)$), as derived in [7], where $a = \ln(2)/d_{cor}$.

$$\Phi_1(\mathbf{f}_T) = \frac{2\pi a}{[a^2 + 4\pi^2 |\mathbf{f}_T|^2]^{\frac{3}{2}}} = \frac{2\pi a}{[a^2 + 4\pi^2 (f_x^2 + f_y^2)]^{\frac{3}{2}}} \quad (9)$$

The 4-D spatial ACF of $\hat{s}(x, y, u, v)$, which corresponds to the JCF in (4), can be evaluated using (10):

$$\begin{aligned} R_s(\Delta x, \Delta y, \Delta u, \Delta v) &= E\{\hat{s}(x, y, u, v)\hat{s}(x + \Delta x, y + \Delta y, u + \Delta u, v + \Delta v)\} \\ &= \sum_{n=1}^N \frac{c_n^2}{2} \cos[2\pi(f_{x,n} \Delta x + f_{y,n} \Delta y + f_{u,n} \Delta u + f_{v,n} \Delta v)] \end{aligned} \quad (10)$$

There are four methods proposed in [11] to determine the spatial frequency set $\{\mathbf{f}_n\}$ and the coefficients $\{c_n\}$ in a SOS model. Three of those methods have been used to model the 2-D shadowing processes [7]. These are the uniform sampling method (USM), the non-uniform sampling method (NUSM) and the Monte Carlo Method (MCM). It is found in [7] that the MCM, where the frequency set $\{\mathbf{f}_n\}$ is generated according to a given *Probability Density Function* (PDF) (which in turn is determined by the PSD), gives the best performance in terms of average square error (ASE) versus the number of sinusoids N . However, this method has the highest computational complexity. The USM method, where the PSD is uniformly sampled with frequency spacing Δf , and $C_n^2/2$ represents the power of the PSD in the frequency interval $[f_n - \Delta f/2, f_n + \Delta f/2]$, requires a large number of sinusoids, but has two features:

- i) The result $\hat{s}(\cdot)$ is a periodical function, which is desirable when the user wants to wrap around the simulated radio environment to avoid interference edge effects.
- ii) It can be implemented using a look-up table based scheme on computer or in hardware (which is fast).

It will be shown later in the analyses of the models that a large number of sinusoids are required to reduce the ASE of a 4-D ACF, even when the MCM method is used; hence a high-speed simulation scheme is necessary. In the rest of this section, we first describe the proposed Discrete Monte-Carlo Method (DMCM), which is a combination of MCM and USM. Following this, a number of performance evaluations are discussed.

C. Discrete Monte Carlo Method

In a pure MCM, the 4-D spatial frequencies set $\{\mathbf{f}_n\}$ in (7) can be generated according to a given joint PDF, which is related to the PSD of the joint shadowing process. Specifically, the sampling frequencies can be generated according to a PDF proportional to the PSD [19]. From (8), it is straightforward that the joint PDF for \mathbf{f} can be decomposed into the two independent identical PDFs for \mathbf{f}_T and \mathbf{f}_R as shown in (11), therefore $\mathbf{f}_{T,n}$ and $\mathbf{f}_{R,n}$ can be generated independently.

$$p_2(\mathbf{f}) = b_2 \Phi_2(\mathbf{f}) = b_2 \Phi_1(\mathbf{f}_T) \Phi_1(\mathbf{f}_R) = b_1 p_1(\mathbf{f}_T) p_1(\mathbf{f}_R) \quad (11)$$

where $p_1(\cdot)$ and $p_2(\cdot)$ denote the 2D and 4D joint PDF functions respectively, and b_1 and b_2 are constants that ensure the integration of the PDF equals to 1. $p_1(\cdot)$ and the functions used to generate $\mathbf{f}_{T,n}$ (the same for $\mathbf{f}_{R,n}$, as they have identical PDFs) have been derived in [7]:

$$|\mathbf{f}_T| = \frac{a}{2\pi} \sqrt{\frac{1}{(1-\beta)^2} - 1} \\ f_x = |\mathbf{f}_T| \cos(\varphi), f_y = |\mathbf{f}_T| \sin(\varphi) \quad (12)$$

where β is a random variable uniformly distributed over the range $[0,1]$, and φ is uniformly distributed over $[0,2\pi]$. θ_n in (7) is a random variable uniformly distributed over $[0, 2\pi]$. The coefficients $\{c_n\}$ have the same value for all sinusoids [11].

To enable an efficient implementation of the MCM, we introduce an equivalent discrete realization of (7), named the Discrete MCM (DMCM). First, letting $2\Delta f$ be the frequency sampling interval as in the USM method, we modify the original sinusoid \mathbf{f}_n from the pure MCM method according to:

$$\tilde{f}_{x,n} = \text{round} \left[\frac{f_{x,n} + \Delta f}{2\Delta f} \right] \cdot 2\Delta f - \Delta f = (2m_{x,n} + 1)\Delta f \quad (13)$$

Where $m_{x,n}$ is an integer. $\tilde{f}_{y,n}$, $\tilde{f}_{u,n}$ and $\tilde{f}_{v,n}$ are modified in the same way as in (13). This modification forces the resulting Gaussian random process to have a period $1/\Delta f$. Then, setting $\Delta\theta = 2\pi/N_{\text{Table}}$ as the resolution of the stored sinusoidal waveform, with table size denoted by N_{Table} , we modify $\{\theta_n\}$ as:

$$\bar{\theta}_n = \text{round} \left(\frac{\bar{\theta}_n - \Delta\theta/2}{\Delta\theta} \right) \cdot \Delta\theta = l_n \Delta\theta \quad (14)$$

where $l_n \in \{0, 1, \dots, N_{\text{Table}}-1\}$. Finally, we set the spatial sampling interval $\Delta x = 1/(N_{\text{Table}} \Delta f)$ and $[\bar{x}, \bar{y}, \bar{u}, \bar{v}] = [k_x, k_y, k_u, k_v] \Delta x$, $k \in \mathbb{Z}$. Equation (7) can then be rewritten in discrete form:

$$\bar{s}(\bar{x}, \bar{y}, \bar{u}, \bar{v}) = \sqrt{\frac{N}{2}} \sum_{n=1}^N \cos \left\{ \frac{2\pi}{N_{\text{Table}}} [(2m_{x,n} + 1)k_x + (2m_{y,n} + 1)k_y \right. \\ \left. + (2m_{u,n} + 1)k_u + (2m_{v,n} + 1)k_v + l_n] \right\} \quad (15)$$

where $\bar{s}(\bar{x}, \bar{y}, \bar{u}, \bar{v})$ is known as a discrete Gaussian random process. It is easy to see from (15) that with $N_{\text{Table}} \rightarrow \infty$, the DMCM becomes a pure MCM when $\Delta f \rightarrow \infty$, or a pure USM when $N \rightarrow \infty$. As all the elements in the operator \sum are in the set $\{\cos(2\pi i/N_{\text{Table}}), i \in \{0, 1, \dots, N_{\text{Table}}-1\}\}$, (15) can be implemented on a computer using a look-up table, with all operations involving only integers; hence simulation speed can be high. According to [14], (15) can be realized on a multiplier-free hardware simulator; however this falls outside the scope of this paper.

In real P2P networks, the shadowing in the uplink and downlink are expected to be identical, i.e. $\hat{s}(x, y, u, v) =$

$\hat{s}(u, v, x, y)$. In order to account for this fact, we introduce the symmetric DMCM. Letting N be even, we first generate the first half of the frequency set $\{\bar{\mathbf{f}}_n\}$, $n=1, 2, \dots, N/2$, as described above. The second half of this set is then generated using:

$$\bar{\mathbf{f}}_{n+N/2} = \bar{\mathbf{f}}_n \cdot \begin{bmatrix} 0 & \mathbf{I} \\ \mathbf{I} & 0 \end{bmatrix}; \quad \mathbf{I} = \begin{bmatrix} 1 & 0 \\ 0 & 1 \end{bmatrix}, n=1, 2, \dots, N/2 \quad (16)$$

i.e. $\bar{\mathbf{f}}_{T,n} = \bar{\mathbf{f}}_{R,n+N/2}$ and $\bar{\mathbf{f}}_{R,n} = \bar{\mathbf{f}}_{T,n+N/2}$ where $n=1, 2, \dots, N/2$. It should be noted that $\bar{\mathbf{f}}_{T,n}$ and $\bar{\mathbf{f}}_{R,n}$ are still independently generated. The above modification makes the discrete spatial frequency set $\{\bar{\mathbf{f}}_n\}$ symmetric with respect to (w.r.t.) $\mathbf{f}_T = \mathbf{f}_R$, which results in a symmetric shadowing value in the up and down links. This will not change the 4-D joint PDF shape since the PDF is symmetric in the same manner (i.e. w.r.t. $\mathbf{f}_T = \mathbf{f}_R$). We also let $\bar{\theta}_n = \bar{\theta}_{n+N/2}$, $n=1, 2, \dots, N/2$. This modification prevents the phase set $\{\bar{\theta}_n\}$ from containing purely random values, and thus introduces additional and unwanted correlations between $\bar{\mathbf{f}}_n$ and $\bar{\mathbf{f}}_{n+N/2}$. Therefore, degradation in performance is expected for the DMCM with symmetric properties (symmetric DMCM) when compared to the non-symmetric approach. The degradation due to the introduction of symmetry is analyzed later in this paper.

D. Performance Evaluation

There are three performance metrics used to evaluate the Gaussian random process simulator: the CDF of the output values, the simulation speed, and the ASE of the ACF. In the DMCM, all the sinusoid frequencies $\{\bar{\mathbf{f}}_n\}$ and $\{\bar{\theta}_n\}$ are randomly generated, hence the above metrics are implementation dependent. However, as mentioned before, when $N \rightarrow \infty$, the DMCM becomes a pure USM, which is then a deterministic model and the ASE for a given sampling frequency resolution (i.e. Δf) can be calculated.

The ASE of an ACF was introduced in [7], and defined as the average squared error between the ACF of the simulated process $\hat{s}(\cdot)$ and the desired ACF of the shadowing processes. It is equal to the square of the root mean square error (RMSE). For joint shadowing processes, the ASE of both the 2-D ACF (ASE_1) and the JCF (ASE_2) have been evaluated using the following definitions:

$$ASE_1 = \frac{1}{XY} \int_{-X/2}^{X/2} \int_{-Y/2}^{Y/2} [R_s(\Delta x, \Delta y) - R_l(\Delta x, \Delta y)]^2 d\Delta x d\Delta y \quad (17)$$

$$ASE_2 = \frac{1}{XYUV} \int_{-X/2}^{X/2} \int_{-Y/2}^{Y/2} \int_{-U/2}^{U/2} \int_{-V/2}^{V/2} [R_s(\Delta x, \Delta y, \Delta u, \Delta v) - R_2(\Delta x, \Delta y, \Delta u, \Delta v)]^2 d\Delta x d\Delta y d\Delta u d\Delta v \quad (18)$$

Since the Gaussian random process generated using the USM is periodic, only the ASE between $[-1/(4\Delta f), 1/(4\Delta f)]$ has to be evaluated. We let $X=Y=U=V=1/(2\Delta f)$ because the 2-D ACF and JCF are symmetric with respect to $X=Y(U=V)$.

For the MCM and the non-symmetric DMCM, the $R_{\hat{s}}(\cdot)$ function can be evaluated using (10). For the symmetric DMCM, (10) is no longer valid and $R_{\hat{s}}(\cdot)$ must be directly evaluated from the generated data. Given a suitable expression for $R_{\hat{s}}(\cdot)$, the ASE can be evaluated using (17) and (18) using numerical integration.

III. NUMERICAL RESULTS

In the following, we present numerical results using the DMCM channel simulation model. The performance of the proposed model with different parameter settings is studied and compared with the pure MCM and USM performance in terms of the ASE of the ACF, the CDF of output values and the simulation speed.

Fig. 1 shows a realization of the symmetric DMCM, where $c_n = \sqrt{2/N}$ to generate a unit power (i.e., $\sum c_n^2/2=1$) Gaussian random process. In order to simulate the shadowing, c_n can be adjusted according to the shadowing standard deviation (in dB). The decorrelation distance is set to 20m, the number of the discrete 4-D spatial sinusoids $N=500$, and the lowest frequency $\Delta f=1/500m$. Hence the period of the output shadowing process is 500m. The sinusoid waveform table size is set to 200. As the discrete frequencies set $\{\bar{f}_n\}$ are symmetric with respect to $f_T=f_R$, only $\bar{f}_{T,n}$ are plotted in the figure. The output sample is generated by defining Tx positions over a 500m x 500m grid with 2m spacings (grid mode) and fixing the Rx at a location in the centre of the test area. The 2-D ACF is evaluated using the data from the grid mode and plotted in Fig. 2, together with the theoretical ACF. To evaluate the JCF, the shadowing data is generated from a route analysis, where both the Tx and Rx move along two straight paths (route mode). The start points and direction of motion for the Tx and Rx are random and independent. Fig. 3 demonstrates the evaluated JCF, which is averaged over the JCFs from 10 route mode studies on one arbitrary DMCM realization.

Fig. 4 and Fig. 5 illustrate the ASE level for the 2-D ACF and JCF respectively. Without loss of generality, the spatial scale is normalized by the decorrelation distance, i.e. $d_{cor}=1$. We vary the number of spatial sinusoids N in the range 100 to 2000, Δf from 1/6 to 1/40, and the table size N_{Table} from 200 to 1000. For the symmetric DMCM, $R_s(\cdot)$ is evaluated directly from the generated data using grid and route mode. The resultant ASEs are averaged over 30 realizations for each method.

It can be seen from Fig. 4 and Fig. 5 that the ASE levels for the 2-D ACF and JCF are similar for a specific method with a given parameter setting, except for the USM. The USM shows a better ASE performance compared to all other methods when Δf is less than 1/20 for the 2-D ACF and 1/15 for the JCF. However, this performance is gained at the cost of an increased number of sinusoids as Δf decreases, e.g. for $\Delta f=1/20$ and a 30dB cut-off frequency f_c (at which the amplitude of PSD in (8) and (9) is 30dB lower than the amplitude at frequency zero), the number of sinusoids is $147^2/2$ for the 2-D Gaussian random process and $46^4/2$ for the 4-D process. The MCM offers the best performance compared to the symmetric and non-symmetric DMCM with the same number of sinusoids N . The ASE improves from 10^{-2} to 10^{-3} when increasing the number of sinusoids from 100 to 500 for both the 2-D ACF and JCF.

The ASE performance of the non-symmetric DMCM is bounded by both the MCM and the USM performance, which is expected since the DMCM is a combination of these schemes. When Δf is greater than 1/10, the ASE level is high and little performance gain is achieved by increasing the number of sinusoids N . This indicates that the performance degradation is mainly due to the large frequency sampling interval. As Δf increases, the ASE level drops and finally hits the ASE level of

the MCM with the same number of sinusoids. For N less than 500, $\Delta f=1/20$ is sufficient for a non-symmetric DMCM to achieve a similar performance to the MCM, while for N greater than 500, a smaller Δf value is required. The reduction of table size N_{Table} from 1000 to 200 is seen to have little effect on the ASE level. However, in a real implementation of the shadowing fluctuation process model, the table size should not be too small since it is inversely proportional to the spatial sampling interval

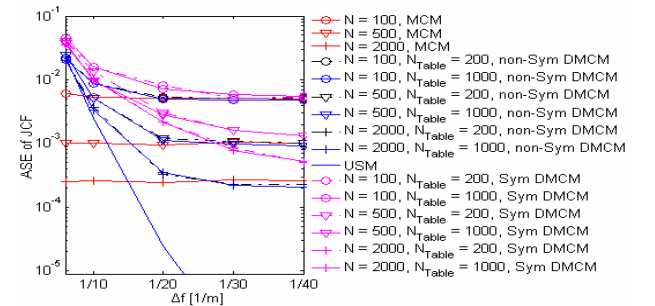
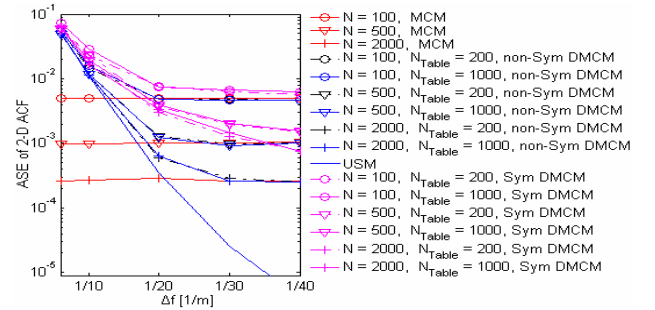
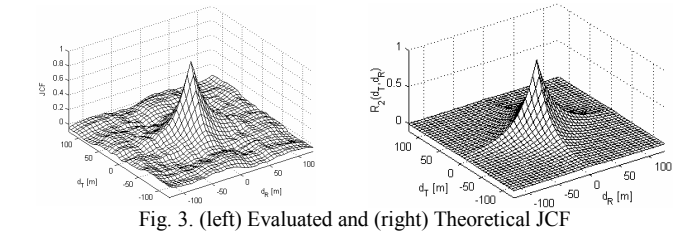
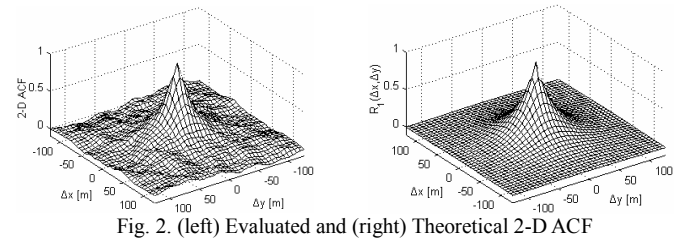
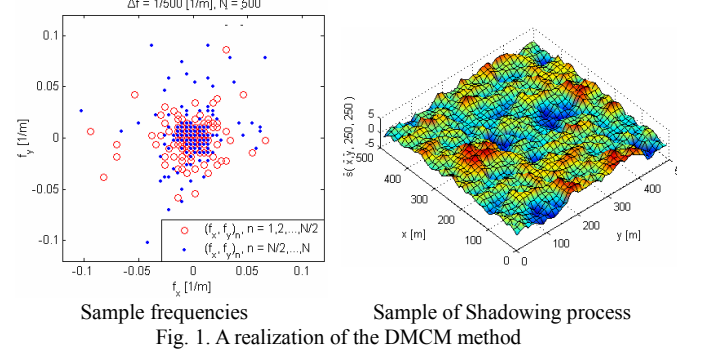


Fig. 4. ASE level of 2-D ACF

Fig. 5. ASE level of JCF

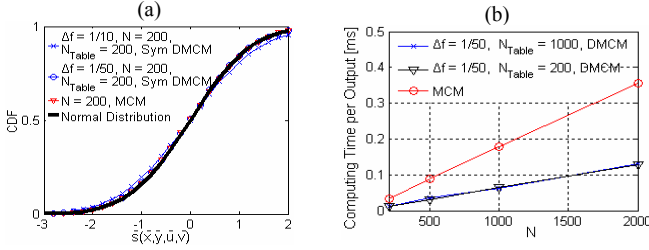


Fig. 6. (a) CDF of the output value (b) Simulation speed comparison

Δx , which must be less than the distance up to which the power values remain approximately constant. An accepted empirical bound is movements over a few tens of a wavelength [17].

Compared to the non-symmetric DMCM with the same parameter settings, the symmetric DMCM has worse ASE performance, which is mainly a result of the additional correlation between \mathbf{f}_n and $\mathbf{f}_{n+N/2}$ caused by introducing symmetry in parameter sets $\{\mathbf{f}_n\}$ and $\{\mathbf{\theta}_n\}$. However, it can be seen from Fig. 4 and Fig. 5 that the degradation in performance can be reduced by increasing the frequency resolution $1/\Delta f$. E.g. with the number of sinusoids $N=100$, the ASE levels of the symmetric DMCM become very close to those of the non-symmetric DMCM when Δf decreases to less than $1/30$. On the other hand, this tendency becomes smaller as N increases.

Fig. 6(a) presents the CDF of the output value from the MCM and DMCM; both evaluated using 10^4 output samples from one arbitrary realization for each method with random Tx and Rx positions. The results show that $N=200$ is adequate to approximate Gaussian process. There is no notable degradation in the CDF performance by increasing Δf from $1/50$ to $1/10$.

Fig. 6 (b) shows the evaluated iteration time (time per output sample) for the pure MCM and DMCM methods, which is an average over 10^5 output samples. The implemented code is written and compiled using C and the computing times are based on a 1.8GHz Pentium 4 processor running Windows XP. As only integer operations are involved in (15), the DMCM is seen to have a speed improvement over the pure MCM. The improvement factor is around 2.8, which is independent of the sinusoid number N , the table size N_{Table} and Δf .

In summary, the MCM approach gives the best performance in terms of ASE versus the number of sinusoids. The ASE level of the proposed DMCM model is bounded by the USM bound when the frequency sampling resolution is low (e.g. Δf is large). The DMCM can achieve the same ASE performance as the MCM when Δf decreases to a certain threshold, which is dependent on the number of sinusoids N . Introducing symmetry degrades the DMCM ASE performance significantly, especially when Δf and N are large. However, a desired ASE level of say $10^{-2.6}$ (corresponding to a mean absolute error of 0.05) can still be achieved by reducing Δf and/or increasing N .

IV. CONCLUSIONS

In this paper, a novel simulation model for the joint shadowing process in urban P2P radio channels has been proposed. The underlying principle is that a Gaussian random process with a given PSD function can be modelled as a sum of sinusoids. The spatial frequencies of the sinusoidal waveforms were determined using a Discrete Monte Carlo Method, which had the following key features:

- 1) The number of sinusoids is relative small (compared to USM).
- 2) The resulting Gaussian process is periodic in the spatial domain.
- 3) Only integer operations are involved in generating the Gaussian random value, and the model can be implemented using a look-up table (enhancing simulation speed).

The DMCM approach offered good simulation speed, with an improvement factor of around 2.8 compared to the pure MCM technique. For most practical parameter settings (with respect to the ASE level), the DMCM method was shown to approximate a Gaussian random process accurately and with significantly reduced simulation time.

ACKNOWLEDGMENT

The authors would like to thank the European Union IST-ROMANTIK Project for financial assistance.

REFERENCES

- [1] 3GPP TR 25.924 V1.0.0. 3GPP TSG-RAN, "Opportunity Driven Multiple Access", Dec. 1999.
- [2] R. Ramanathan, J. Redi, "A Brief Overview Of Ad Hoc Networks: Challenges And Directions" IEEE Comm. Magazine, May, 2002
- [3] J. Vidal, et al. "Multihop networks for capacity and coverage enhancement in TDD/UTRAN", MedHocNet, Sardinia, Sep. 2002.
- [4] N. Patwari, Y. Wang, and R. J. O'Dea, "The importance of the multipoint-to-multipoint indoor radio channel in ad hoc networks," in IEEE Wireless Commun. and Networking Conf., Orlando, Mar. 2002
- [5] M. Gudmundson, "Correlation model for shadow fading in mobile radio systems," Electron. Lett., vol. 27, pp. 2145–2146, Nov. 1991.
- [6] A. Gehring, M. Steinbauer, I. Gaspard, and M. Grigat, "Empirical channel stationarity in urban environments," EPMCC, Feb. 2001
- [7] X. Cai, G. Giannak, "A Two-Dimensional Channel Simulation Model for Shadowing Processes", IEEE Trans. Veh. Technol., Vol.52, Nov. 2003
- [8] H. Kim, Y. Han, "Enhanced Correlated Shadowing Generation in Channel Simulation", IEEE COMMUNICATIONS LETTERS, VOL. 6, NO. 7, JULY 2002
- [9] Fabio Graziosi, Fortunato Santucci, "A General Correlation Model for Shadow Fading in Mobile Radio Systems" IEEE COMMUNICATIONS LETTERS, VOL. 6, NO. 3, MARCH 2002
- [10] ftp://ftp.3gpp2.org/TSGC/Working/2003/3GPP2_3GPP2_SCM, Spatial Channel Model Text Description v7.0, 3GPP2, August 19, 2003
- [11] M. Pätzold, U. Killat, F. Laue, "A deterministic digital simulation model for Suzuki processes with application to a shadowed Rayleigh land mobile radio channel," IEEE Trans. Veh. Technol., vol.45, May 1996.
- [12] M. Pätzold and F. Laue, "Statistical properties of Jakes' fading channel simulator," VTC'98, vol. II, Ottawa, ON, Canada, May 1998,
- [13] M. Pätzold, U. Killat, F. Laue, and Y. Li, "On the statistical properties of deterministic simulation models for mobile fading channels," IEEE Trans. Veh. Technol., vol. 47, Feb. 1998.
- [14] M. Pätzold, R. Farcia, and F. Laue, "Design of high-speed simulation models for mobile fading channels by using table look-up techniques," IEEE Trans. Veh. Technol., vol. 49, July 2000.
- [15] S. O. Rice, "Mathematical analysis of random noise," Bell Syst. Tech. J., vol. 23, pp. 282–332, July 1944.
- [16] Z. Wang, E. K. Tameh, A. R. Nix, O. Gasparini "A Joint Shadowing Process Model for Multihop/Ad-hoc Networks in Urban Environments", WRF11, 2004
- [17] L. M. Correia, "Wireless flexible personalized communications, COST 259: European co-operation in mobile radio research" ISBN 0471 49836X, pp.77-222, 2001
- [18] W. C. Y. Lee, "Mobile Communications Engineering". New York: McGraw Hill, 1982
- [19] P. Höher, "A statistical discrete-time model for the WSSUS multipath channel," IEEE Trans. Veh. Technol., vol. 41, pp. 461–468, Nov. 1992.